# New micromegas detectors in the CAST experiment

## (CERN Axion Solar Telescope)

S. Aune[2] H. Brauninger[3] T. Dafni[1] G. Fanourakis[4] E. Ferrer Ribas[2]
J. Galán Lacarra[1] T. Geralis[4] I. Giomataris[2] F. Iguaz[1] I.G. Irastorza[1]
K. Kousouris[4] J. Morales[1] J.P. Mols[4] T. Papaevangelou[2] M. Pivovaroff[6]
J. Ruz[1] R. Soufli[6] A. Tomás Alquézar[1] K. Zachariadou[4]

[1] Laboratorio de Física Nuclear y Astropartículas, Zaragoza, Spain
[2] DAPNIA, Centre d'etudes de Saclay, Gif sur Yvette CEDEX, France
[3] Max-Planck-Institut fur extraterrestrische Physic, Garching, Germany
[4] Institute of Nuclear Physics, NCSR Demokritos, Athens, Greece
[5] Institute fur Kernphysik, TU-Darmstadt, Darmstadt, Germany
[6] Lawrence Livermore National Laboratory, 7000 East Avenue, Livermore, USA

8th International Conference on Position Sensitive Detectors, 2008

# Outline

# Outline

# Introduction

- CAST uses an LHC prototype (dipole) superconducting magnet mounted on a rotating platform.
- The magnet can follow the Sun's center during sunset and sunrise during more than 1.5 hours.
- The magnet operates at a temperature around $1.8K$.
- Transverse magnetic field $B = 9.0T$ inside the two magnet bores with $L = 9.26m$.
- 4 x-ray detectors : x-ray telescope (mirror optics and CCD) + 3 $\mu M$ detectors.

The axion is a pseudo scalar Nambu-Goldstone boson that can be produced via Primakoff effect in stellar plasmas (e.g. Sun)

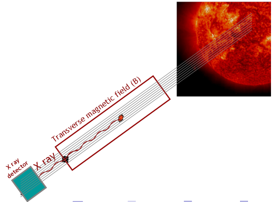


- Phase I (Vacuum) : $m_a < 0.02eV$ (2003-2004)
- Phase II (He4) : $m_a < 0.38eV$ (2005-2006)
- Phase II (He3) : $m_a < 1.15eV$ (2008-2010?)

# The theoretical axion signal

- The axion solar flux was calculated by *G. Raffelt* using the well understood Standard Solar Model.
- The prediction places the main axion signal in the $2-7keV$ range.
- The axion converts into an x-ray photon in presence of an intense magnetic field.

- The conversion probability decreases *drastically* with the q-transfered of the process.
- A buffer gas is needed ($m_\gamma > 0$) inside the *cold bore* to recover sensitivity in higher masses.

$$q = \frac{m_a^2 - m_\gamma^2}{2E_a}$$

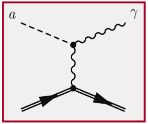


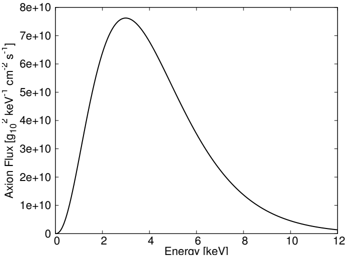


## Axion

- The axion comes out as the most elegant solution to the CP-violation problem (*Peccei-Quinn* 1977)
- The axion has low mass, is elec. neutral and weakly interacting with normal matter -> *Dark matter candidate*.

# He3 Phase Upgrade

- New He3 recovery system and advanced He transfer.
- New $\mu M$ vacuum line (detector pressure and flow control).
- 2 new sunset $\mu M$ detectors replacing the old TPC detector.
- Added shielding for the sunrise detector.
- Improved shielding from the old TPC detector to the sunset side.

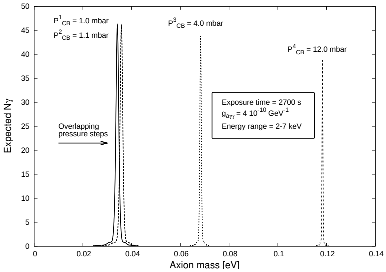


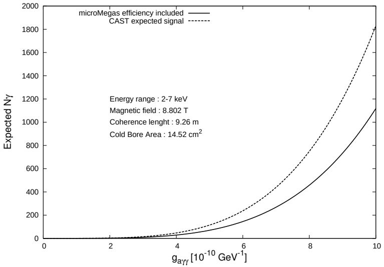


- During data taking the gas is transfered to the cold bore in the middle of the tracking.
- 2 daily pressure steps are measured.

- The sensitivity of CAST depends strongly in the low background rate of the detectors.

# Outline

# CAST

## New micromegas detectors

- The latest generation of Micromegas detectors are in production for CAST.
- Detectors are built with low radiation materials (Plexiglass, Kapton, ...)

### Bulk

- 30$\mu m$ inox mesh.
- 128$\mu m$ pilars.
- 3-4 years of experience : well established technique.
- Reachable energy resolution (18%$FWHM$ ).
- Spatial uniformity and very robust.
- Limit on the energy resolution due to the thickness of the mesh.

### Microbulk

- 5$\mu m$ copper mesh.
- 30$\mu m$ mesh holes.
- pilars are replaced by attached Kapton substrate.
- 1-2 years of experience : technology almost complete.
- Reachable energy resolution ($<$ 13%$FWHM$ ).
- Fragility to sparks.

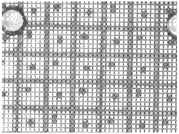

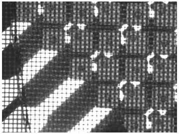

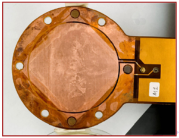

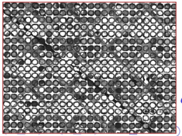

# CAST

## Sunrise detector installation

- New vacuum line + detector pressure and flow control
- Designed a new lead + cadmium + cupper shielding for the new line.
- Polythylene shielding designed to optimize space and weight limitation.
- Inner shielding flooded with nitrogen (Radon contamination and water vapor reduction).

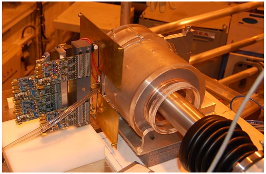

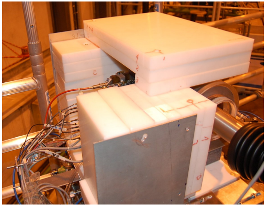

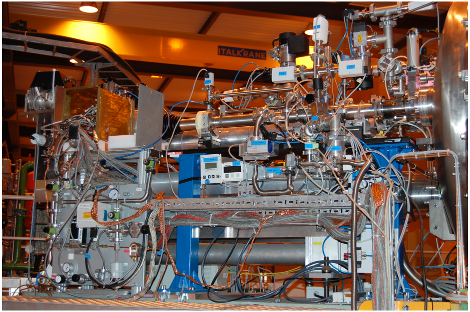

# CAST

## Sunset detectors

- Replacement of the sunset TPC by 2 micromegas detectors (1 bulk + 1 microbulk).
- Great background reduction *x*15: Better events discrimination and new TPC shielding design.

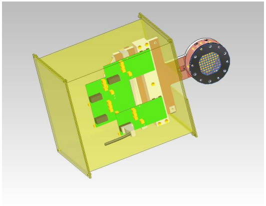

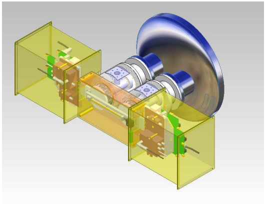

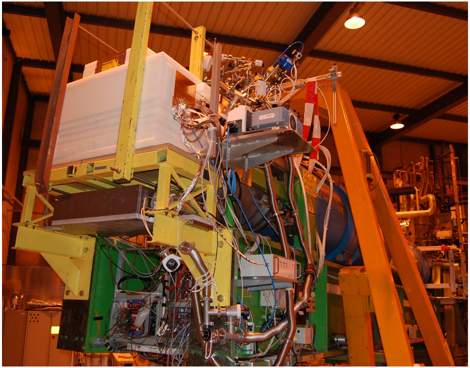

# Outline

# Micromegas in CAST

Expected signal and detectors efficiency.

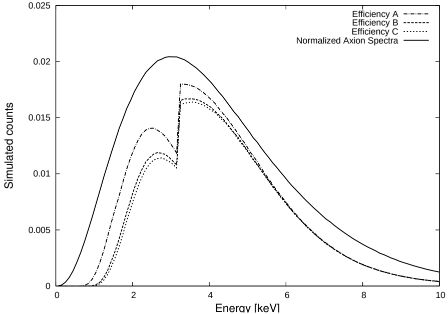


| Overal efficiency (2-7 keV) | | |
|---|---|---|
| A | mM detector | 75.97 % |
| B | mM + CW | 62.45 % |
| C | mM + CW + DW | 61.49 % |

## Sunrise detector efficiency loss contributions

- Intrinsic detector efficiency (Argon).
- 5 $\mu m$ Aluminised-mylar drift window + 5% Strongback
- 4 $\mu m$ polypropylene differential window
- 15 $\mu m$ polypropylene cold window + 17.5% Strongback

## Sunset detectors efficiency loss contributions

- Intrinsic detector efficiency (Argon).
- 5 $\mu m$ Aluminised-mylar drift window + 5% Strongback
- 15 $\mu m$ polypropylene cold window + 17.5% Strongback

# Micromegas in CAST

## Sunrise detector stability

- New bulk detector (B4) was installed at the beginning of July.
- A Fe55 calibration is taken after tracking to check stability and apply rejection.

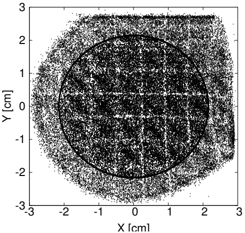


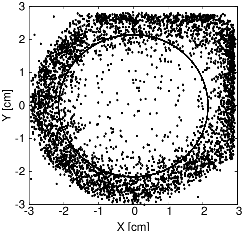


- Mesh voltage is reduced the 22nd of July.
- Background level evolves to a constant rate.

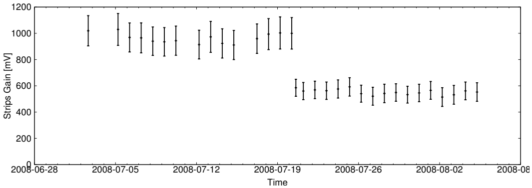


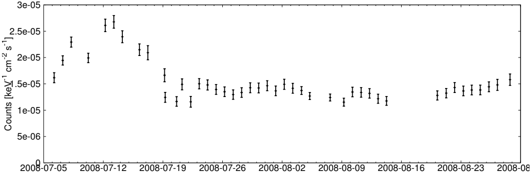

# Micromegas in CAST

## Sunrise detector gain stability

- Sunrise detector frontal calibration allows to study the gain distribution evolution.
- Gain is uniform through all the detection area.

| Energy resolution (FWHM) | 28.45% |
|---|---|
| Gain standard desviation | 1.4% |

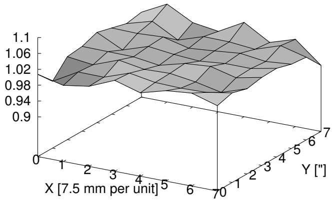


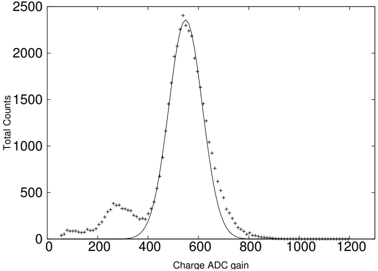


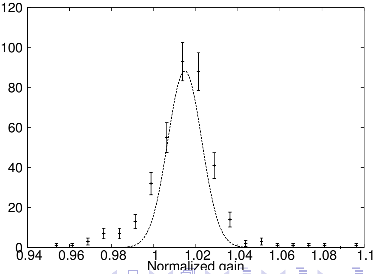

# Micromegas in CAST

## Sunset detectors stability

### Microbulk detector

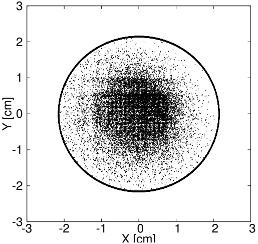


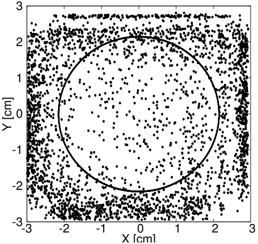


- Sunset detectors are calibrated from the back every 8 hours.

### Bulk detector

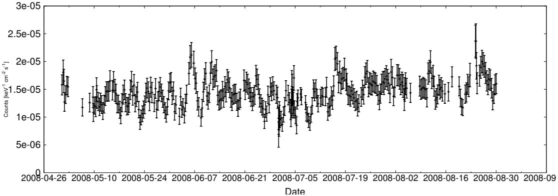


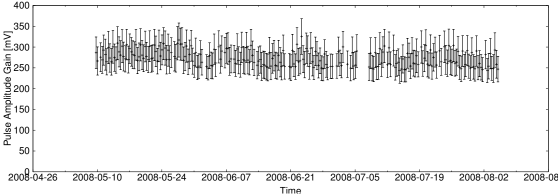

# Outline

# Micromegas data analysis

## Micromegas readout

- Mesh signal comes from ions produced in the amplification gap.
- Electron avalanches created in the amplification gap give a signal in the strips.
- The temporal mesh pulse and the spatial strips provide good information for event discrimination.

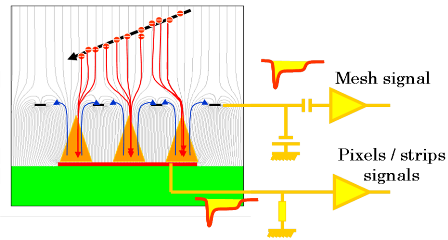


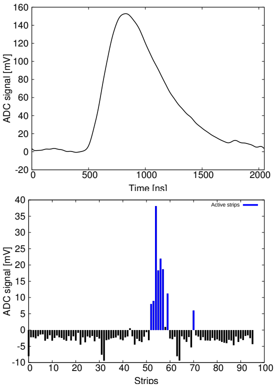

# Modified Standard Multivariate Method (K.Kousouris)

- A covariance matrix is built for ($E_o = 5.96keV$).
- The q-value is transformed to include energy dependence.

$$q' = q_o \cdot \left(\frac{E}{E_o}\right)^a$$

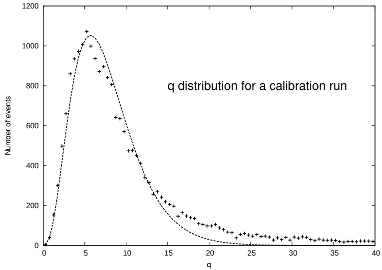


$$f_q(q) = \frac{1}{2^{N/2}\Gamma(N/2)} q^{N/2-1} e^{-q/2}$$

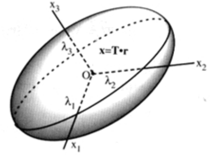


## Observables used for background discrimination

- Risetime-Width ratio
- Energy balance
  - Strips
  - Pulse Integral
  - Pulse Amplitude
- Cluster X-Y energy balance
- Cluster multiplicity balance
- Cluster skew

# Micromegas data analysis

## Neural Networks method

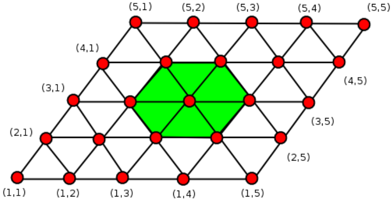


- A Neural network is trained using background data.
- After training each cell identifies events with different parameters.
- A calibration run determines which cells are the x-ray photon sensitive ones.

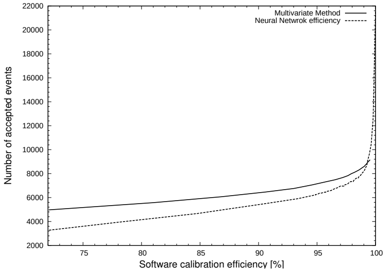


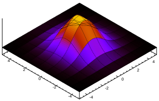

The weights of each cell are the observables coming from *pulse* and *strips*.

$$w_{ik} = w_{ik} + \alpha(t) \cdot h(d_{ig}, R(t)) \cdot (x_k - w_{ik})$$

# Micromegas data analysis

## Background level

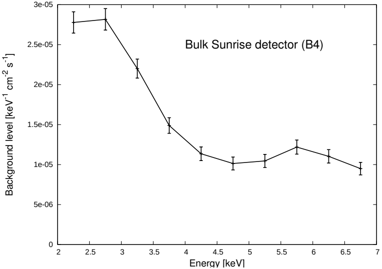


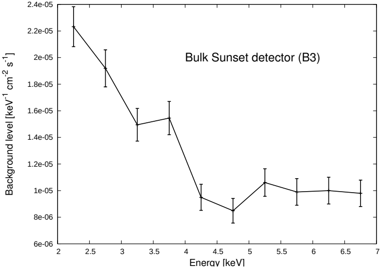


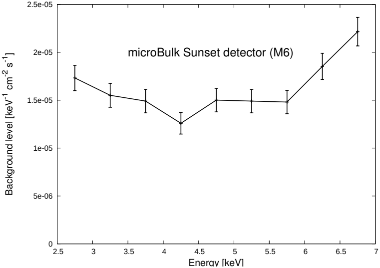


| Background level | |
|---|---|
| Sunrise (B4) | $1.20 \cdot 10^{-5}$ |
| Sunset (B3) | $1.42 \cdot 10^{-5}$ |
| Sunset (M6) | $1.76 \cdot 10^{-5}$ |

- Sunrise micromegas background level is reduced by a factor 3 for the new He3 Phase.

# Outline

# Micromegas detectors characterization

## Bulk detector (I)

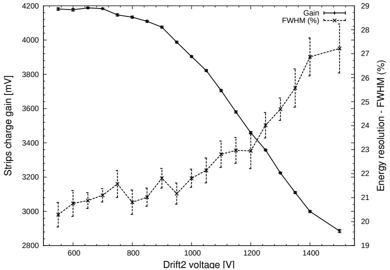


- Bulk detector was fully characterised in Saclay.
- Valuable data for finding the optimum setup and improve the discrimination analysis.

## Detector evolution with

- Pressure.
- Isobutane concentration.
- Drift voltage.
- Mesh voltage.

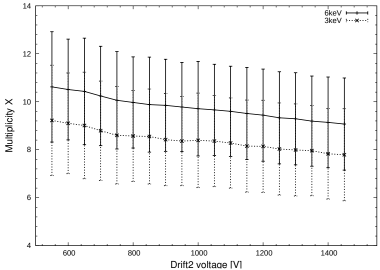

# Micromegas detectors characterisation

## Bulk detector (II)

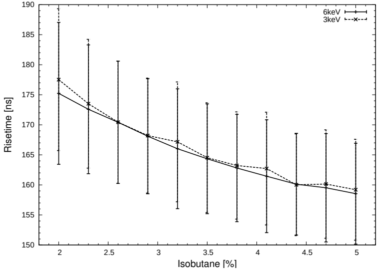


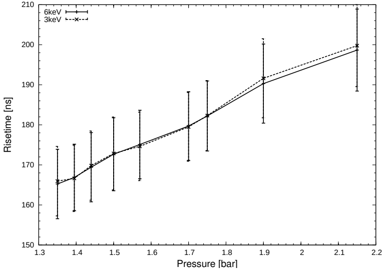


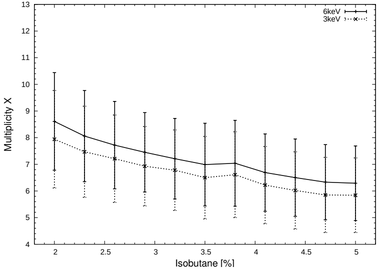


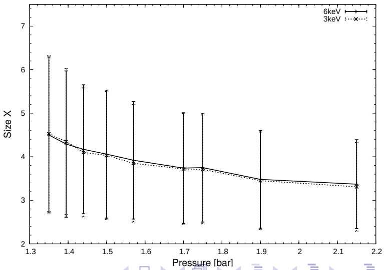

# Outline

# Micromegas detectors characterisation

## Microbulk detector

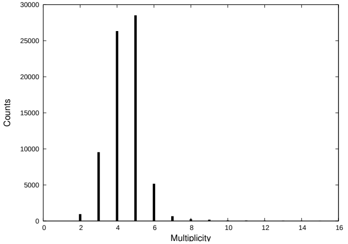


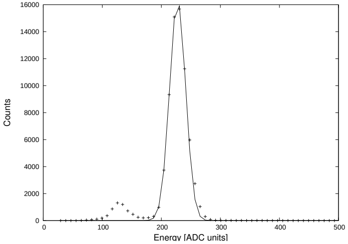


- Last microbulk detector (M9) tested in CEA Saclay.
- Energy resolution for this measurement 13.99% FWHM.
- Good spatial resolution and cluster behaviour.

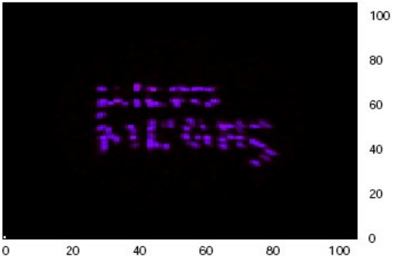

# Micromegas detectors characterisation

## Energy characterization in CAST


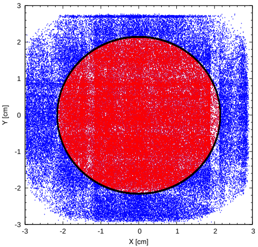


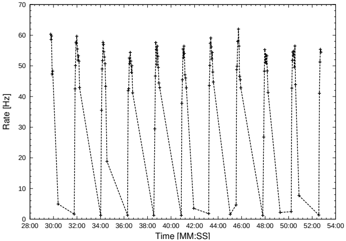


- An x-ray generator installed in the sunset side is used to crosscheck the alignment of the x-ray telescope.
- The sunset Microbulk detector is able to detect scattering from the walls.
- The x-ray energies cover the full energy range of the detector.
- Allows frontal characterization *in situ*.

# Micromegas detectors characterisation

## Calibration in energy

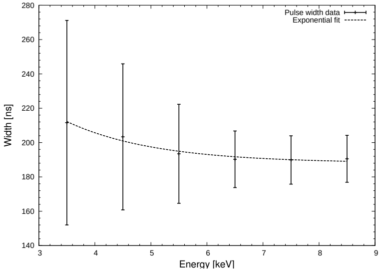


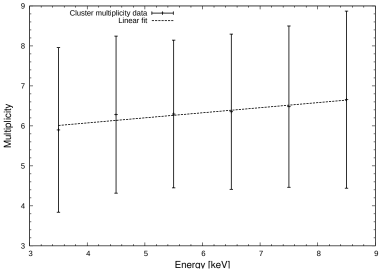


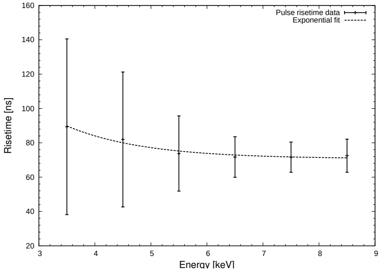


- Pulse parameters and cluster size are found to be slightly dependent with the x-ray energy.
- Corrections to be included in discrimination analysis.
- Covariance matrix is now parametrizable with energy.

# Conclusions and prospects

- Micromegas detectors have shown good performance and stability for the long data taking periods of the CAST experiment.
- Last micromegas detectors are robust to the mechanical vibrations during CAST magnet movement.
- Stable background rate : 3 $\mu M$ detectors with similar background levels.
- The micromegas detector will detect the first axions!

- New spare detectors for further testing and characterization.
- Background measurements will be carried out in *Canfranc Underground Laboratory* to complete the last detectors characterizations.
- More accurate energy measurements to be done in x-ray facilities.
- It is expected to improve even more the low background level of the new detectors by optimizing the setup and data analysis.
- The last characterizations will increase the reliability of the background data, and will reduce the effect of systematics.